

## STABILITY OF HIGH-COERCIVITY STATE OF Nd-Fe-B SINTERED MAGNETS PREPARED WITH DyH<sub>2</sub> ADDITIONS

BURKHANOV Gennadij S.<sup>1</sup>, KOLCHUGINA Natalia B.<sup>1</sup>, DORMIDONTOV Andrey G.<sup>2</sup>, LUKIN Alexander A.<sup>2</sup>, SITNOV Vladimir V.<sup>2</sup>, KOSHKID'KO Yurij S.<sup>3,4</sup>, SKOTNICOVÁ Kateřina<sup>4</sup>, ČEGAN Tomáš<sup>4</sup>

<sup>1</sup>*Baikov Institute of Metallurgy and Materials Science, Russian Academy of Sciences, Moscow, Russian Federation*

<sup>2</sup>*JSC SPETSMAGNIT, Moscow, Russian Federation*

<sup>3</sup>*International Laboratory of High Magnetic Fields and Low Temperatures, Polish Academy of Sciences, Wrocław, Poland, EU*

<sup>4</sup>*VSB - Technical University of Ostrava, Faculty of Metallurgy and Materials Engineering, Regional Materials Science and Technology Centre, Ostrava, Czech Republic, EU*

### Abstract

The effect of low-temperature treatment on the structure and hysteretic properties of sintered Nd-Fe-B magnets, which were prepared using strip-casting alloy (wt.%) Nd - 24%, Pr - 6.5%, Dy - 0.5%, B - 1%, Al - 0.2%, Fe - balance and 2 wt.% DyH<sub>2</sub> addition, was studied. Hysteretic properties of the magnets subjected to the optimum heat treatment (1-h holding at 500 °C followed by quenching in gaseous nitrogen) are  $B_r = 1.29$  T,  $jH_c = 1309$  kA·m<sup>-1</sup>,  $H_k = 1220$  kA·m<sup>-1</sup>,  $(BH)_{max} = 322$  kJ·m<sup>-3</sup>. The subsequent combined heat treatment in vacuum or inert atmosphere, which includes the stepped or progressive heating from 250 to 500 °C (the total heating time is to 20 h), does not change hysteretic properties of magnets upon heating within this temperature range, whereas magnets of the same composition, but prepared by traditional technology, demonstrate the abrupt decrease of hysteretic properties ( $jH_c$  and  $H_k$ ) upon heating in a temperature range of 350 to 400 °C. The degradation of magnetic properties (decrease in  $jH_c$  and  $H_k$  to 1105 and 960 kA·m<sup>-1</sup>, respectively) of magnets prepared from hydride-containing powder mixtures is observed only after the repeated annealing at 550 °C. The hysteretic properties of the magnets can be restored completely by heat treatment 1050 °C (1 h) + 500 °C (2 h). X-ray diffraction analysis and scanning electron microscopy were used to demonstrate the evolution of microstructure and phase composition of magnets in the course of annealings.

**Keywords:** Nd-Fe-B-based magnets, coercivity, dysprosium hydride, low-temperature annealing, grain boundaries

### 1. INTRODUCTION

Sintered Nd-Fe-B magnets find wide applications for technology owing to the high maximum energy product ( $(BH)_{max}$ ), residual inductance ( $B_r$ ), and magnetization coercive force ( $jH_c$ ). Nd-Fe-B permanent magnets are used in many fields of industry. One of problems of preparation of permanent magnets based on the Nd<sub>2</sub>Fe<sub>14</sub>B compound is related to the decrease in the content of nonmagnetic phases via the optimization of the rare-earth metals contents [1].

The coercivity of Nd-Fe-B magnets is structure sensitive and dependent on the continuity and composition of RE-rich phases, grain-boundary defects, average grain size, exchange interaction between Nd<sub>2</sub>Fe<sub>14</sub>B hard magnetic grains, etc. The coercivity of sintered magnets is reached by post-sintering annealing at the optimum temperature (around 500 °C) determined by the composition of Nd-Fe-B-based alloys. The role of the low-temperature heat treatment (LTHT) consists in the formation of continuous non-magnetic RE-rich layers between (Nd,R)<sub>2</sub>(Fe,M)<sub>14</sub>B grains [2].

According to [1, 3], the addition of heavy rare earths of Dy or Tb is effective to enhance the coercivity and consequent thermal stability of the Nd-Fe-B magnets, because Dy or Tb increases the magnetic anisotropy field of the 2-14-1 Nd-Fe-B compound, but this method simultaneously results in considerable degradation of the remanence of the magnets. Recently, techniques for enhancement of coercivity of sintered Nd-Fe-B magnets by diffusing a continuous layer of Dy or Tb onto the surface of the Nd<sub>2</sub>Fe<sub>14</sub>B matrix grains without obvious reduction of the remanence have been developed by different researchers.

The experiments with Dy and Tb additions are carried out to achieve the optimum microstructure, which involves confining the Dy distribution to the grain boundary regions. If the Dy can be confined in the grain boundary regions, then:

- (1) It should be possible to increase locally the coercivity and hence reduce the probability of reverse domains forming at the grain boundaries.
- (2) Limit the substitution of Nd by Dy in the matrix phase and thus limit the reduction of the magnetization and hence the remanence.
- (3) Reduce the amount of Dy required to achieve a particular increase in the coercivity and hence reduce the overall cost of the alloy.

The magnetic and microstructural modification of the Nd-Fe-B sintered magnet by mixed DyF<sub>3</sub>/DyH<sub>x</sub> powder doping was studied in [4].

According to [5], magnets based on Nd<sub>16</sub>Fe<sub>76</sub>B<sub>8</sub> with DyH<sub>3</sub> additions have been sintered at different temperatures. The magnetic properties, microstructure and compositions have been examined. Details of progress of Dy entering the hard matrix phase are considered and an evolution mode of the relevant sintering process is proposed. Hydrogen absorption and desorption of the magnets were examined by HDTA. The optimum sintering temperature for these magnets has been established. Microstructural and EDX examinations have revealed that a relatively Dy-rich phase formed in the Nd-rich grain boundary phase and this slowed down the substitution of Nd by Dy in the Nd<sub>2</sub>Fe<sub>14</sub>B matrix phase, possibly enhancing local coercivity without excessive attenuation of the remanence.

The effect of DyH<sub>3</sub> additions on the magnetic properties of magnets was studied in [6]. The use of DyH<sub>x</sub> powder along with DyGa, Dy<sub>3</sub>Co powders allows the authors to increase the coercive force by 0.4 to 0.6 T without substantial decrease in the residual magnetization. The DyH<sub>x</sub> powder was prepared by hydrogenation of metallic Dy at 500 °C at a hydrogen pressure of 500 kPa. The powder was applied on the Nd-Fe-B magnet surface and annealed in a vacuum at 550 °C for 0.5 h.

The possibility of application of dysprosium hydride nanoparticles for wastes processing is discussed in [7]. The properties of prepared magnets are:  $B_r = 1.296$  T,  $jH_c = 1360$  kA·m<sup>-1</sup>,  $(BH)_{max} = 292.3$  kJ·m<sup>-3</sup>.

The present work is aimed at the study of peculiarities of both the formation high-coercivity state of Nd-Fe-B magnets prepared from DyH<sub>2</sub> hydride-containing powder mixtures and the evolution of hysteretic properties of the magnets in the course of low-temperature annealings.

## 2. EXPERIMENTAL

Nd-Fe-B magnets were prepared using Nd - 24 wt.%, Pr - 6.5 wt.%, Dy - 0.5 wt.%, B - 1 wt.%, Al - 0.2 wt.%, Fe - 65.8 wt.% strip-casting alloy. The preparation procedure includes the hydrogen decrepitation of flakes in dry hydrogen (at 100 °C for 1 h) and subsequent passivation in gaseous nitrogen atmosphere. Dysprosium hydride (2 wt.%) was added after cooling the powder to room temperature. The mixture was subjected to fine milling for 40 min to an average particle size of 3 μm using a vibratory mill and isopropyl alcohol medium. Samples were compacted in a magnetic field and sintered at T = 1070 °C (for 2 h). The sintered blanks were subjected to the following heat treatments (HTs):

- **HT-1** (optimum): 500 °C (1 h) + quenching in gaseous nitrogen (Sample No.1);

- **HT-2:** 500 °C (1 h) + quenching + 500 °C (2h) + quenching + 500 °C + cooling for 2 h to 400 °C + 400 °C (6 h) + furnace cooling (in this case, the properties are almost unchanged, although the earlier experiments performed for similar magnets demonstrates the decrease in magnetic properties  $jH_c$  and  $H_k$ ) (Sample No.2);
- **HT-3:** 500 °C (1 h) + quenching + 500 °C (2h) + quenching + 500 °C + cooling for 2 h to 400 °C + 400 °C (6 h) + furnace cooling + 550 °C (1h) + quenching (properties decreases substantially) (Sample No.3);
- **HT-4:** HT-1 + HT-2 + HT-3 + 1050°C + 500 °C (2 h) + quenching in gaseous nitrogen (hysteretic properties of the magnets restored completely) (Sample No.4).

Measurements of magnetic characteristics were performed at room temperature using a closed circuit of hysteresisgraph and samples 40 mm in diameter and 8 mm thick, which were subjected to HT-1, HT-2, HT-3 and HT-4.

The X-ray diffraction analysis of “strip-casting” alloy and sintered magnets was performed using a Difrei 401 diffractometer and  $CrK_{\alpha}$  radiation. The structural studies were carried out using samples demagnetized in a vacuum at 775 K to recovery the initial state.

X-ray diffraction patterns were processed using PowerCell software. This program allows one to simulate X-ray diffraction patterns using crystal structure parameters of a compound, crystal lattice sizes, atomic positions in the crystal lattice and X-ray wavelength.

The complex microstructure and phase composition of samples were investigated by SEM/EDX using a Quanta 450 FEG microscope.

### 3. RESULTS AND DISCUSSION

#### 3.1. Magnetic properties

Hysteretic properties of the studied magnets are given in **Table 1** and **Fig. 1**. The temperature of the optimum HT equal to 500 °C is likely to be determined by the maximum wettability of grain-boundary  $R_{rich}$  [8] ensuring continuous 2-14-1-phase grain boundaries (sample No.1) (**Fig. 1a**). The subsequent combined heat treatment in vacuum or inert atmosphere, which includes the stepped or progressive heating from 250 to 500 °C (the total heating time is to 20 h), does not change the hysteretic properties of magnets (sample No.2) (**Fig. 1a**). As was noted above, magnets of the same composition, but prepared by traditional technology, demonstrate the abrupt decrease of hysteretic properties ( $jH_c$  and  $H_k$ ) upon heating in a temperature range of 350 to 400 °C. The degradation of magnetic properties (decrease in  $jH_c$  and  $H_k$  to 1105 and 960  $kA \cdot m^{-1}$ , respectively) of magnets prepared from hydride-containing powder mixtures is observed only after the repeated annealing at 550 °C (sample No.3) (**Fig. 1b**). The annealing at 970 °C for 1 h does not restore the hysteretic properties. The hysteretic properties of the magnets can be restored completely by heat treatment 1050 °C (1 h) + 500 °C (2 h) (sample No.4) (**Fig. 1a**).

**Table 1** Hysteretic properties of the studied magnets.

Quantity	Sample Nos.1, 2, 4	Sample No.3
$B_R$ (T)	1.29	1.26
$H_{CM}$ ( $kA \cdot m^{-1}$ )	1309	1105
$H_{CB}$ ( $kA \cdot m^{-1}$ )	981	895
$H_K$ ( $kA \cdot m^{-1}$ )	1262	888
$(BH)_{max}$ ( $kJ \cdot m^{-3}$ )	322	303

The degradation and recovery of properties are discussed from the point of view of (1) formation and dissolution of impurity  $\text{Nd}_{1.1}\text{Fe}_4\text{B}_4$  phase at triple junctions of 2-14-1 magnetic phase, (2) changes of grain boundaries; (3) presence of oxide phases at triple junctions; and (4) existence of compositional nonuniformity of 2-14-1 magnetic phase grains.

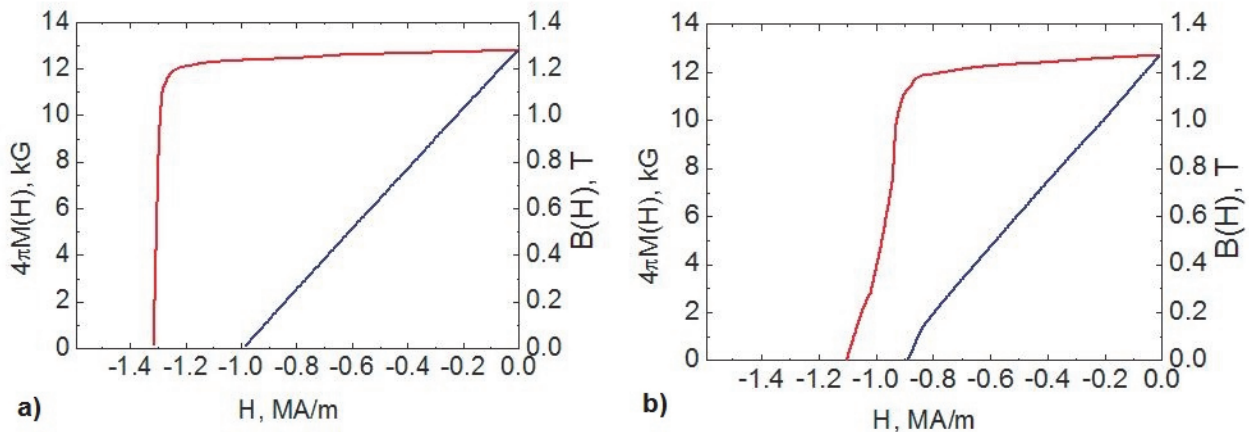


**Fig. 1** Demagnetization curves for samples after (a) optimum (sample No.1), stepped (sample No.2) and restoring (sample No.4) HTs, (b) degrading HT (sample No.3)

### 3.2. X-ray diffraction analysis

The degradation and recovery of properties are discussed from the point of view of formation and dissolution of impurity  $\text{Nd}_{1.1}\text{Fe}_4\text{B}_4$  phase at triple junctions of 2-14-1 magnetic phase, changes of grain boundaries; presence of oxide phases at triple junctions; and existence of compositional nonuniformity of 2-14-1 magnetic phase grains.

**Fig. 2 (a, b, c)** shows portions of X-ray diffraction patterns of samples subjected to optimum HT (sample No.1) (**Fig. 2a**), degrading HT (sample No.3) (**Fig. 2b**) and restoring HT (sample No.4) (**Fig. 2c**), which demonstrate the evolution of the  $\text{NdO}$ ,  $\text{Nd}_2\text{O}_3$  and  $\text{Nd}_{1.1}\text{Fe}_4\text{B}_4$  phases in the magnets in the course of HTs. **Fig. 2** demonstrates comparison of experimental X-ray diffraction pattern (black line) and pattern simulated for the  $\text{Nd}_2\text{Fe}_{14}\text{B}$ -type structure (space group  $P42/mnm$ ) (red line). It is seen that main reflections simulated for the  $\text{Nd}_2\text{Fe}_{14}\text{B}$  coincide adequately with those in the experimental X-ray diffraction pattern; some reflections are likely to belong to other phases. These reflections are observed at  $2\Theta$  angles of 46.01; 46.42; 53.58 and 79.13 deg. Subsequent analysis of experimental X-ray diffraction patterns was performed in detail using literature data and simulated X-ray diffraction patterns. It is known from literature that the presence of  $\alpha$ -Fe phase can affect the properties of permanent magnets. However, we failed to detect the  $\alpha$ -Fe phase at the background of reflections of the  $\text{Nd}_2\text{Fe}_{14}\text{B}$  phase. Based on the analysis of chemical composition and literature data, we assumed the presence of REM oxide phases in ternary junctions of samples under study. According to literature data, ternary junctions can contain different oxide phases. These are  $\text{NdO}$  with the NaCl-type structure (space group  $Fm-3m$ ) (the oxygen content is 50 at.%),  $\text{Nd}_2\text{O}_3$  with the  $\text{La}_2\text{O}_3$ -type structure (space group  $Pm-3m$ ) (the oxygen content is 60 at.%), and  $\text{NdO}_2$  with the  $\text{CaF}_2$ -type structure (space group  $Fm-3m$ ) (the oxygen content is 67 at.%).

Results of simulation of X-ray diffraction patterns are shown in **Fig. 2** by red line. As is seen from these figures, patterns simulated for the structures of the  $\text{NdO}$  and  $\text{Nd}_2\text{O}_3$  oxides agree adequately with experimental patterns. A slight difference can be explained by the fact that the simulation was performed for the  $\text{NdO}$  and  $\text{Nd}_2\text{O}_3$  compounds, whereas, according to chemical analysis data, these compounds can contain Dy and Pr, i.e., can differ from the composition preset with the simulation program.

The X-ray diffraction pattern for sample No.3 exhibits a small peak at  $2\Theta = 42.7$  deg. along with the other aforementioned reflections. We assumed that this reflection corresponds to the  $\text{Nd}_{1.1}\text{Fe}_4\text{B}_4$  phase. The

evolution of the peak after restored annealing allows us to state the decomposition of the phase.

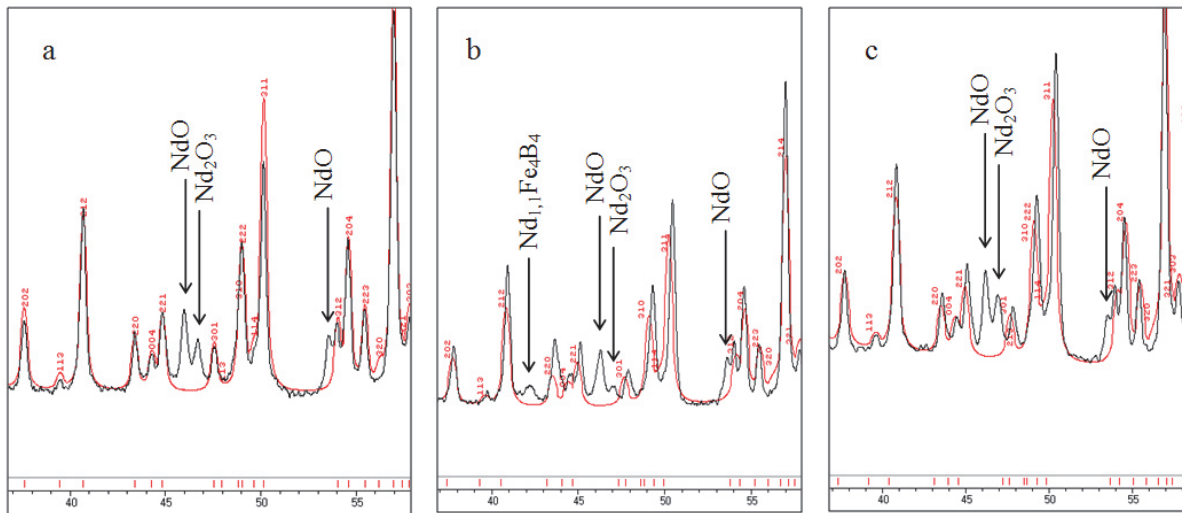


**Fig. 2** Part of the X-ray diffraction pattern for samples after (a) optimum (sample No.1), (b) degrading (sample No.3) and (c) restoring (sample No.4) HTs ( $\lambda = 0.22909$  nm). Red line corresponds to simulated pattern for the  $\text{Nd}_2\text{Fe}_{14}\text{B}$ -type structure

### 3.3. Study of grain boundaries

**Fig. 3** shows images taken with the magnification 20000x. To decrease the image blur, the scanning time was increased. These figures demonstrate transformations of grain boundaries during degrading and restoring HTs, which cause the formation of discontinuous and continuous boundaries, respectively.

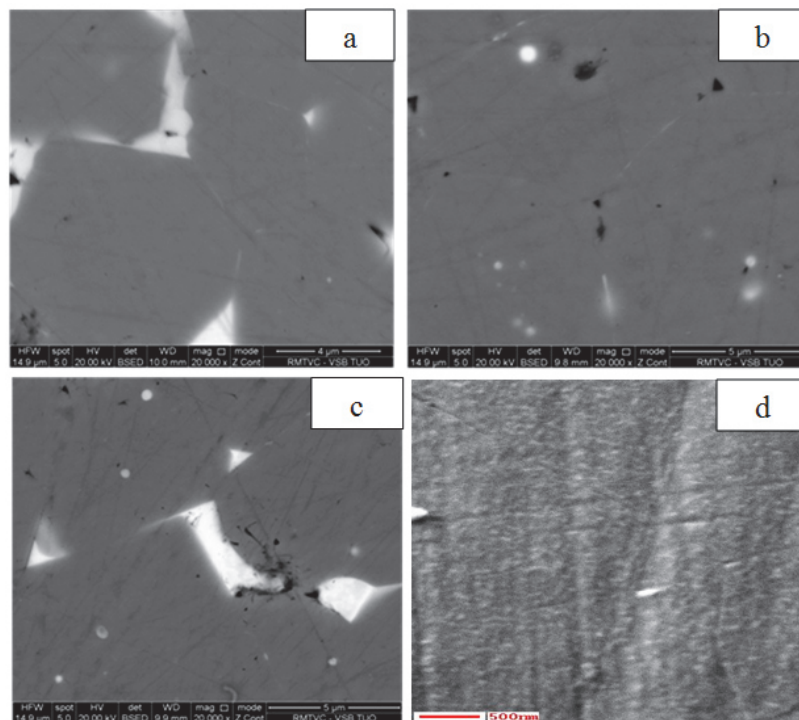


**Fig. 3** SEM image of the surface of samples after (a) optimum (sample No.1), (b) stepped (sample No.2), (c) degrading (sample No.3) and (d) restoring (sample No.4) HTs

The absence of any changes in  $jH_c$  and  $H_k$  after HTs at 250-500 °C is likely can be related to the substantial decrease in the invar effect (anomalous temperature dependence of the lattice parameters), which is due to magnetic ordering [9,10] at the expense of 2-14-1 phase structuring (**Fig. 3c**) [11].

As is evident from **Fig. 3**, grain boundaries are seen clearly for samples nos. 1, 2 and 4. The structure of grain boundaries in sample No. 3 is discontinuous and in some areas, grain boundaries are almost vanishes (or invisible). In [12], the effect of annealing temperature on the state of grains boundaries and magnetic properties of Nd-Fe-B magnets was studied. It was shown that discontinuous grain boundaries lead to a decrease in the coercive force. As mentioned above, grain boundaries are formed by a paramagnetic R-rich phase.

Layer R-rich phase provides magnetic isolation of grains. This increases the resistance to demagnetization grain. Therefore, if there are more smooth grain boundaries, the coercive force of the permanent magnets is increased. However, in our case, to conclude definitely the effect of state of grain boundaries on the coercive force, additional studies by high-resolution microscopy should be performed.

#### 4. CONCLUSION

Samples of high-coercivity (Nd,Pr)-Fe-B magnets were prepared using powder mixtures containing DyH<sub>2</sub>. The effect of low-temperature treatments of the magnetic properties of developed magnets was studied by X-ray diffraction analysis and electron microscopy. Conditions of the optimum low-temperature heat treatment were determined. Compositions of paramagnetic phases formed at triple junctions of 2-14-1 phase grains were determined; the phases are (Nd,Pr,Dy)-O and Nd<sub>1.1</sub>Fe<sub>4</sub>B<sub>4</sub>. Evolution of the phases during low-temperature treatments and their effect on magnetic properties, in particular, on the coercive force of magnets is discussed. The used binary mixtures technology has allowed us to obtain the higher coercive force magnitude as compared to that of magnets prepared by traditional technology.

The data obtained demonstrate the higher thermal stability of hysteretic properties of magnets prepared from hydride-containing powder mixtures. The observed effect is attributed to the formation of a non-uniform Dy distribution in (Nd, Pr, Dy)<sub>2</sub>Fe<sub>14</sub>B principal magnetic phase grains, which is formed during the preparation of material from hydride-containing powder mixtures and determines the specificity of diffusion processes occurred during low-temperature annealing. These data are of importance for deciding the optimum heat treatment of Nd-Fe-B-based magnets and the prediction of their service stability.

#### ACKNOWLEDGEMENTS

*This study was supported by the ERA\_NET\_RUS\_PLUS, project no. INNO\_146 and Russian Academy of Science, Branch of General Chemistry (program no. 5) and created in terms of project No. LO1203 „Regional Materials Science and Technology Centre - Feasibility Program” funded by Ministry of Education, Youth and Sports of Czech Republic.*

#### REFERENCES

- [1] KOLCHUGINA N., LUKIN A., BURKHANOV G. S., SKOTNICOVÁ K., DRULIS H., PETROV V. Role of terbium hydride additions in the formation of microstructure and magnetic properties of sintered Nd-Pr-Dy-Fe-B magnets. In Metal 2012: 21<sup>th</sup> International Conference on Metallurgy and Materials. May 23<sup>rd</sup>-25<sup>th</sup> 2012 Brno, Czech Republic. Ostrava: Tanger s.r.o., 2012, pp. 1387-1392.
- [2] SEPERHRI-AMIN H., OHKUBO T., HONO K. The mechanism of coercivity enhancement by the grain boundary diffusion process of Nd-Fe-B sintered magnets. Acta Materialia, Vol. 61, No. 2013, pp. 1982-1990.
- [3] LIU W.Q., SUN H., YI X.F., LIU X.C., ZHANG D.T., YUE M., ZHANG J.X. Coercivity enhancement in Nd-Fe-B sintered permanent magnet by Dy nanoparticles. Journal of Alloys and Compounds, Vol. 501, No. 1, 2010, pp. 67-69.
- [4] TAE-HOON KIM, SEONG-RAE LEE, HYO-JUN KIM, MIN-WOO LEE, AND TAE-SUK JANG. Magnetic and micro-

- structural modification of the Nd-Fe-B sintered magnet by mixed DyF<sub>3</sub>/DyH<sub>x</sub> powder doping. *Journal of Applied Physics*, Vol. 115, No. 17, 2014, pp. 17A763.
- [5] GAOLIN YAN, MCGUINNESS P.J., FARR J.P.G., HARRIS I.R. Optimisation of the processing of Nd-Fe-B with dysprosium addition. *Journal of Alloys and Compounds*, Vol. 491, No. 1-2, 2010, L20-24.
- [6] POPOV A.G., VASILENKO D.YU., PUZANOVA T.Z., SHITOV A.V., VLASYUGA A.V. Effect of diffusion annealing on hysteretic properties of sintered Nd-Fe-B magnets. *The Physics of Metals and Metallography*, Vol. 111, No. 5, 2011, pp. 471-478.
- [7] LIU W.Q., LI C., ZAKOTNIK M., YUE M., ZHANG D.T., ZUO T.Y. Waste Nd-Fe-B sintered magnets recycling by doping with DyH<sub>3</sub> nanoparticles. In *Proceeding REPM2014*, 2014, pp. 116-118.
- [8] WOODCOCK T. G., GUTFLEISCH O. Multi-phase EBSD mapping and local texture analysis in NdFeB sintered magnets. *Acta Materialia*, Vol. 59, No. 3, 2011, pp. 1026-1036.
- [9] ANDREEV A. V., DERYAGIN A. V., ZADVORKIN S. M., TERENCEV S. M. Thermal expansion and spontaneous magnetostriction of R<sub>2</sub>Fe<sub>14</sub>B (R = Y, Nd, Sm) compounds. *Fizika tverdogo tela*, Vol. 27, No. 6, 1985, pp. 1641-1645.
- [10] BUSCHOW K. H. J. Invar effect in R<sub>2</sub>Fe<sub>14</sub>B compounds (R = La, Ce, Nd, Sm, Gd, Er). *Journal of the Less Common Metals*, Vol. 118, No. 2, pp. 349-353.
- [11] LUKIN A. A., KOL'CHUGINA N. B., BURKHANOV G. S., KLYUEVA N. E., SKOTNITSEVA K. Role of Terbium hydride additions in the formation of microstructure and magnetic properties of sintered Nd-Pr-Dy-Fe-B magnets. *Inorganic Materials: Applied Research*, Vol. 4, No. 3, 2013, pp. 256-259.
- [12] VIAL F., JOLY F., NEVALAINEN E., SAGAWA M., HIRAGA K., PARK K.T. Improvement of coercivity of sintered NdFeB permanent magnets by heat treatment. *Journal of Magnetism and Magnetic Materials*, Vol. 242-245, 2002, pp. 1329-1334.